doi: 10.15407/ujpe61.06.0561

A. NAUMENKO,[1] L. KULIKOV,[2] N. KONIG[2]

[1] Taras Shevchenko National University of Kyiv
(64/13, Volodymyrs'ka Str., Kyiv 01601, Ukraine)
[2] Frantsevich Institute for Problems of Materials Science, Nat. Acad. of Sci. of Ukraine
(3, Krzhizhanovs'kyi Str., Kyiv 03680, Ukraine)

RAMAN SPECTRA OF GRAPHENE-LIKE NANOPARTICLES OF MOLYBDENUM AND TUNGSTEN DISULFIDES

PACS 78.40.Me, 78.55, 78.67.Bf, 78.67.Sc

The Raman spectra obtained in the case of graphene-like 2H-MoS_2 and 2H-WS_2 nanoparticles and depending on their average sizes in the [013] and [110] crystallographic directions are reported. It is established that the Raman spectra of graphene-like 2H-MoS_2 nanoparticles and micron particles are closely related. Similarities of the Raman spectra point to the homogeneity of graphene-like 2H-MoS_2 nanoparticles. The small shifts and the Raman spectrum line widening, for graphene-like 2H-MoS_2 and 2H-WS_2 nanoparticles, which are caused by the influence of the sizes of nanoparticles and their anisotropy, have been observed. The dependence of Raman spectra of graphene-like 2H-MoS_2 nanoparticles on the their size in the crystallographic direction [110] is first shown, i.e. the positions of bands in the spectrum depend not only on the number of nanolayers S-Mo-S, but also on the size in the [110] direction.

Keywords: MoS_2, WS_2 layered materials, graphene-like materials, Raman spectroscopy, vibrational-electronic interaction.

1. Introduction

Due to their unusual electronic structures and exceptional physical properties, two-dimensional (2D) layered nanomaterials have attracted much attention in recent years [1–12]. Graphene, a single-layer 2D carbon material with zero band gap, is the most studied 2D nanomaterial and shows extensive applications because of its fascinating properties such as the high electron mobility, good thermal conductivity, excellent elasticity, and mechanical stiffness [4, 5, 7, 9]. Recently, the layered transition metal dichalcogenides (2H-MX_2, M = Mo, W, X = S, Se) arosed also a considerable interest due to their unique physical properties such as the ideal band gap and a large in-plane electron mobility [1–3, 5, 6, 8].

Raman spectroscopy has been very successful in the study of phonons and their couplings to electrons in 2D crystals like graphene in few-layer regime [13–15]. The probing of interlayer phonons through Raman spectroscopy is challenging, since these phonon modes are usually of very low frequencies (several to tens of wavenumbers) and difficult to be distinguished from the Rayleigh background scattering.

From the analysis of the numerous recent publications on graphene-like 2H-MX_2, mainly 2H-MoS_2, it follows that the main attention of researchers was focused on the study of the Raman spectrum features as functions of the number of nanolayers obtained, as a rule, by the micromechanical exfoliation of 2H-MoS_2 single crystals.

The results of Raman spectroscopy are widely used as the evidence of the homogeneity of 2H-MoS_2 and 2H-WS_2 nanostructures (nanolayers, nanosheets). Small shifts and the Raman spectrum line widening depending on the number of layers for graphene-like 2H-MoS_2 and 2H-WS_2 nanoparticles (nanolayers, nanosheets) have been observed in several works (see, e.g., [16-25]). Nevertheless up to date, no specific features of the Raman spectra of graphene-like 2H-MoS_2 and 2H-WS_2 nanoparticles depending on the number of layers and/or their average size anisotropy (in [013] and [110] crystallographic directions) are studied. This limits the wider application of Raman spectroscopy for the attestation of 2D nanomaterials based on graphene-like 2H-MX_2, in particu-

lar, in relation to the features of their real nanostructures and the surface states studied by other methods. It should be noted that the differences in the Raman spectra of graphene-like layers of 2H-MoS_2 and 2H-WS_2 nanoparticles described in the literature have been obtained by different methods. As a result, the possible inconsistency of the spectra may be due to the lack of the homogeneity of samples, the influence of different dangling chemical bonds at the edges of flat nanoparticles of different lengths and thicknesses, especially in the real nanostructures (ordered nanostructures, partial or complete their disorder), and surface conditions, which requires a further research.

In this connection, our purpose is to establish the features of Raman spectra of graphene-like 2H-MoS_2 and 2H-WS_2 nanoparticles depending on the anisotropy of their average sizes in the crystallographic directions [013] and [110].

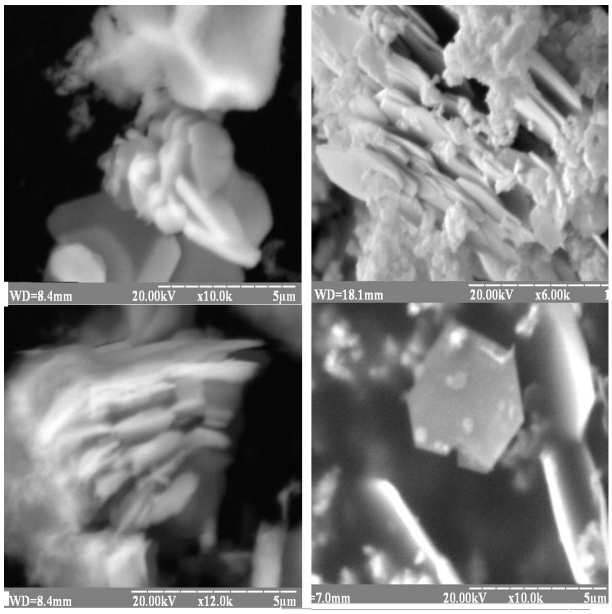

Fig. 1. SEM of graphene-like 2H-MoS_2 (left) and 2H-WS_2 (right) nanoparticles

2. The Experimental Details

The laboratory nanotechnology of the preparation of graphene-like 2H-MoS_2 and 2H-WS_2 nanoparticles was developed within the Chemical Vapor Deposition (CVD) method. This nanotechnology enable one to prepare graphene-like 2H-MoS_2 or 2H-WS_2 nanoparticles in sufficient amounts, which are homogeneous by the chemical composition (2H-MoS_2 or 2H-WS_2), type of layered structure (2H-MoS_2 that is characteristic of appropriate micron powders and single crystals), form of nanostructures (2D, graphene-like nanoparticles), average sizes of anisotropic nanoparticles (extremely small sizes of the order of 1 nm for the [013] crystallographic direction) and do not contain impurities of foreign phases including X-ray amorphous ones and other nanostructures. Average sizes of anisotropic 2H-MoS_2 nanoparticles are adjusted effectively in wide ranges (for [013] and [110] crystallographic directions; X-ray and SEM data): $d_{[013]}$ = 2.7(2)–4.7(2) nm, $d_{[100]}$ = 8.5(4)–53(3) nm. The minimum number of S–Mo–S nanosheets (coaxial to the Z axis, i.e., the c parameter of a unit cell) for 2H-MoS_2 nanoparticles is 4 – by evaluation data (nanosynthesis "bottom-up", layer-by-layer self-assembly of S–Mo–S nanosheets). Average sizes of anisotropic 2H-WS_2 nanoparticles are adjusted effectively in wide ranges too (for [013] and [110] crystallographic directions; X-ray and electron microscopy data): $d_{[013]}$ = 2.8(2)–75(5) nm, $d_{[100]}$ = 7.9(4)–123(8) nm. The minimum number of S–W–S nanosheets for 2H-WS_2 nanoparticles is 4–12 by the evaluation of data. The samples of graphene-like 2H-MoS_2 and 2H-WS_2 nanoparticles, which were taken for the investigations, are collected in Table 1. The examples of SEM for graphene-like 2H-MoS_2 and 2H-WS_2 nanoparticles are shown in Fig. 1, *a* and *b*. Their micron powders were also used for comparison.

Raman spectra were detected by an automated double spectrometer DFS-24 ("LOMO", Russia) equipped with a cooled photomultiplier and a registration system that operates in a photon counting mode. The backscattering geometry has been used in the experiments. The light source was a linearly polarized, cylindrical focused 514.5-nm Ar^+-laser and a 633-nm He–Ne laser. A cylindrical lens was used to focus light into a 10×0.1 mm^2 spot. It is worth to mention that the larger illuminated area can efficiently eliminate the local heterogeneity (more reliable data) and minimize the probability of the radiation damage of a sample due to the resonance adsorption. In order to obtain a more reliable information, the additional technique was applied to minimize the noise. In particular, the relatively wide spectral win-

Table 1. **X-ray data of graphene-like 2H-MoS_2 and 2H-WS_2 nanoparticles**

Compound	Seq. number	Unit cell parameters, nm		Average sizes of nanoparticles for [013] and [110] crystallographic directions, nm		Number of layers
		a	c	d[013]	d[110]	
2H-MoS_2	1	0.31601 (1)	1.22984 (6)	>200	>200	–
	2	0.31621 (4)	1.2294 (7)	4.2 (2)	17 (1)	6
	3	0.31600 (5)	1.2255 (7)	4.7 (2)	43 (3)	8
	4	0.31622 (5)	1.2254 (8)	3.9 (2)	53 (3)	6
2H-WS_2	5	0.31521 (2)	1.2365 (1)	>200	>200	–
	6	0.31522 (2)	1.2374 (1)	7.1 (4)	27.8 (9)	10
	7	0.31517 (2)	1.2359 (2)	57 (4)	76 (5)	92
	8	0.3152 (2)	1.2540 (2)	2.8 (2)	102 (9)	4

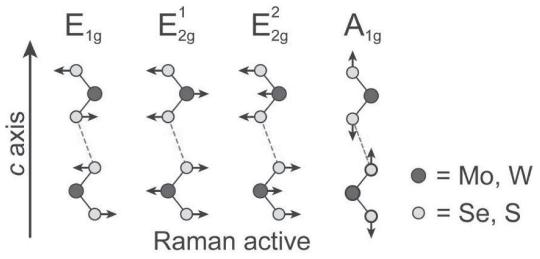

Fig. 2. Schematic drawing of four Raman active modes of the transition metal dichalcogenides (2H-MX_2, M = Mo, W and X = Se, S)

dows of about 3–5 cm^{-1}, long acquisition time, and optimized digital averaging of the spectra with a variable spectral window were used for the amplification of weak signals.

3. Results and Discussion

It is known that layered 2H-MX_2 (M = Mo, W; X = S, Se) are composed of hexagonal close-packed weakly bonded S–Mo–S single layers. Each layer, henceforth referred to as "trilayer", consists of three atomic layers (two hexagonal planes of S atoms and an intercalated hexagonal plane of Mo atoms bound with S atoms in a trigonal prismatic arrangement) covalently bonded to one another, and the adjacent trilayers are coupled via the weak van-der-Waals interaction. The investigated 2H-MX_2 compounds (2H-MoS_2 and 2H-WS_2) are of the most common 2H type. The crystal structure of 2H-MX_2 is described by $P6m1$ (D^4_{6h} point group). There are 18 lattice vibrational modes at the point Γ of the center of the Brillouin zone. The distribution of fundamental vibrational modes over the irreducible representations of zone center ($k = 0$) phonons are as follows [26, 27]: $\Gamma = A_{1g}+2A_{2u}+B_{1u}+2B_{2g}+E_{1g}+2E_{1u}+E_{2u}+2E_{2g}$, among which only A_{1g}, E_{1g}, and $2E_{2g}$ are Raman active modes. The atomic displacement of these four Raman active modes is shown in Fig. 2.

The A_{1g} mode is an out-of-plane (breathing) vibration involving only the chalcogen atoms in the direction along the c-axis, while the two-fold degenerate E-symmetry modes involve the in-plane (shear) displacement of M and chalcogen atoms [20, 21]. The E^2_{2g} mode is a shear mode corresponding to the vibration of two rigid layers against each other and appears at very low frequencies (<50 cm^{-1}) [20, 21, 23, 25–27].

The space group of a 2H-MX_2 monolayer is $P6m2$ (point group D_{3h} [X]. There are 9 modes at the Brillouin zone center [25, 28]. The Γ phonons can be expressed by the irreducible representations: $\Gamma = 2A''_2+A'_1+2E'+E''$, where A''_2 and E' are acoustic modes, A''_2 is IR active, A'_1 and E'' are Raman active, and another E' is both Raman and IR active. The rigid layer shear mode E^2_{2g} is absent in monolayers [29].

The unpolarized Raman spectrum of bulk 2H-WS_2 obtained with the 473-nm excitation shows the characteristic A_{1g} and E^1_{2g} peaks that are clearly separated and have similar intensities. In contrast, only one prominent peak can be clearly seen in the bulk 2H-WS_2 spectrum in the frequency region, where we expect A_{1g} and E^1_{2g} peaks [23].

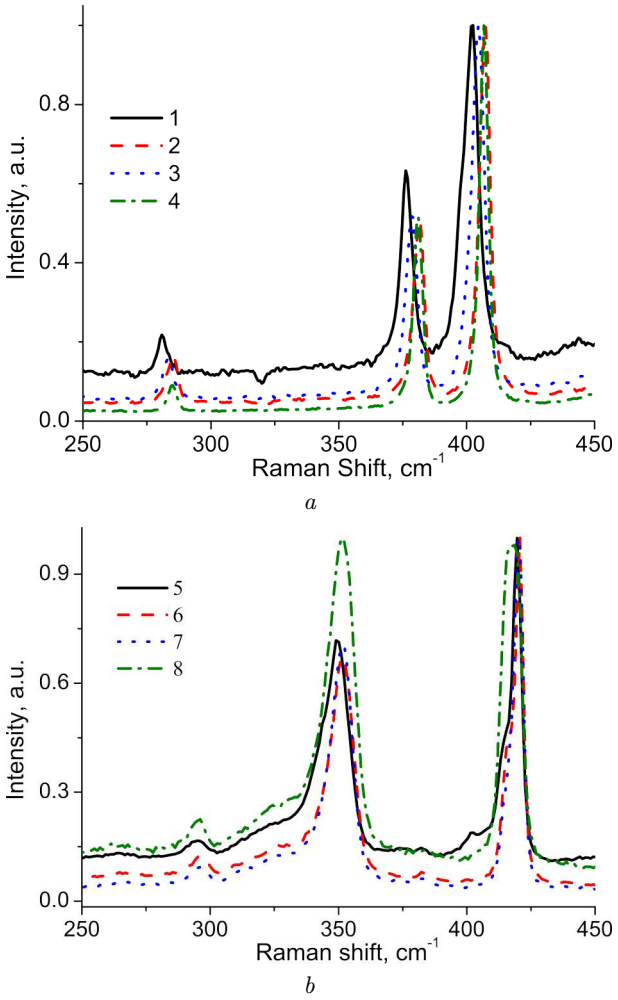

Fig. 3. Raman spectra of graphene-like 2H-MoS_2 nanoparticles (curves *2–4*) and micron particles of natural 2H-MoS_2 (curve *1*) according to Table 1 (samples 1–4) (*a*) and Raman spectra of graphene-like 2H-WS_2 nanoparticles (curves *6–8*) and micron particles of natural 2H-WS_2 (curve *5*) according to Table 1 (samples 5–8) (*b*)

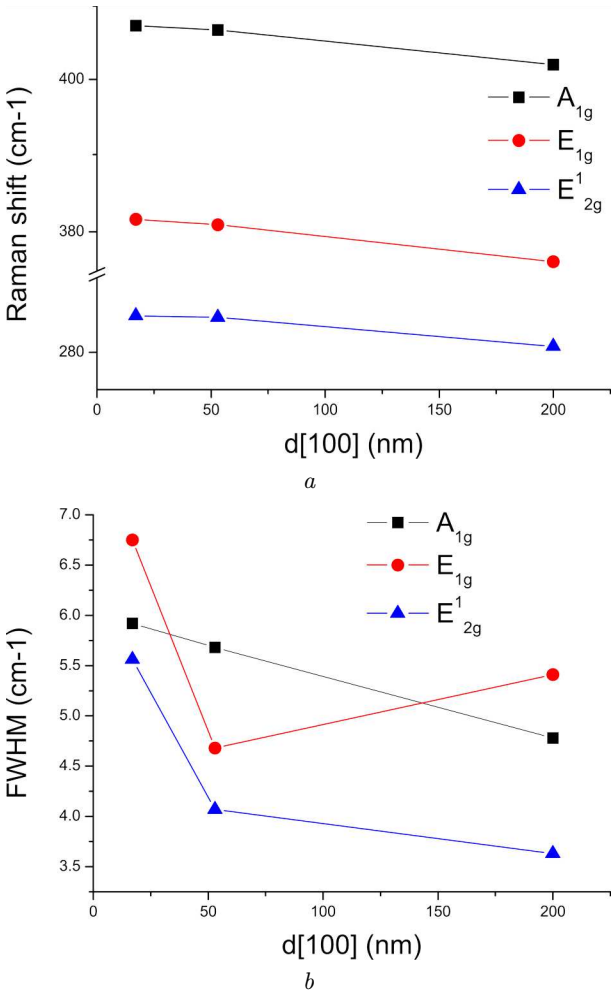

Fig. 4. The spectral positions of lines in the Raman spectra of graphene-like 2H-MoS_2 nanoparticles and micron particles of natural 2H-MoS_2 (*a*) and the FWHM of corresponding lines (*b*) depending on the particle sizes in the bazal plane

The Raman spectra of graphene-like 2H-MoS_2 and 2H-WS_2 nanoparticles (see Table 1) and their micron powders for comparison are presented in Figs. 3, *a* and 3, *b*. The spectra are normalized and vertically offset for clarity.

Both in-plane E^1_{2g} at 383 cm^{-1} and out-of-plane A_{1g} at 409 cm^{-1} modes have been observed for a micron 2H-MoS_2 powder (see Fig. 3, *a*, curve *1*) in good agreement with the previous studies [30–34].

For a micron 2H-MoS_2 powder, the shifts of the spectral positions of these modes to 376 cm^{-1} and 402 cm^{-1}, respectively, are detected. Indeed, some low-intensity bands in the spectral interval 240—450 cm^{-1} with bands at 281 cm^{-1} and 402 cm^{-1}, respectively, (curve *1*, Fig. 3, *a*) are found. These bands shift to 283 cm^{-1} (curve *3*, Fig. 3, *a*) and 285 cm^{-1} (curves *2* and *4*, Fig. 3, *a*), by depending on the average sizes of graphene-like 2H-MoS_2 nanoparticles. As an example, the experimental data on the spectral positions and the full widths at half-maximum (FWHM) of Raman bands in the Raman spectra of graphene-like 2H-MoS_2 nanoparticles as functions of their sizes in bazal plane $d_{[110]}$ are collected in Table 2 and illustrated in Fig. 4.

Table 2. **Dependence of the Raman shifts and the FWHM for graphene-like 2H-MoS_2 nanoparticles on their sizes in bazal plane $d_{[110]}$**

Raman mode	Raman shift/FWHM		
	17 nm	53 nm	200 nm
A_{1g}	407.3 (5.9)	406.7 (5.7)	402 (3.8)
E_{1g}	381.6 (6.8)	380.9 (4.7)	376.2 (5.4)
E^2_{2g}	284.9 (5.6)	284.7 (4.1)	280.8 (3.6)

Thus, in the case of graphene-like 2H-MoS_2 nanoparticles, the dependence of Raman shifts on the nanoparticle size in the crystallographic direction [110] has been investigated for the first time, i.e. the shifts of the Raman spectra of nanoparticles 2H-MoS_2 depend not only on the number of nanolayers S–Mo–S, but also on the size in the [110] direction.

The same picture was observed for graphene-like 2H-WS_2 nanoparticles, but band shifts are not such illustrative, as in case of 2H-MoS_2 nanoparticles, possibly, due to the larger atomic masses. Two maxima in the high-frequency region, whose position changes from 421 cm^{-1} to 417 cm^{-1} and 352—349.5 cm^{-1} with the average sizes of graphene-like 2H-WS_2 nanoparticles are found. The spectra in the region 150—300 cm^{-1} are much richer than in the case of 2H-MoS_2 nanoparticles. As is seen from Fig. 3, *b*, the maxima at 349.6 and 419.6 cm^{-1} (sample 5 in Table 1, curve *1* in Fig. 3, *b*), 351.6 and 420.7 (sample 6 in Table 1, curve *2* in Fig. 3, *b*), 351.7 and 417 cm^{-1} (sample 7 in Table 1, curve *3* in Fig. 3, *b*) have been observed for micron powder of 2H-WS_2.

The closeness of the Raman spectra of micron and nano graphene-like 2H-MoS_2 and 2H-WS_2 shows the homogeneity of the latter, by confirming the results of our previous X-ray and electron microscopic studies. It should be emphasized that, according to X-ray diffraction studies, 2H-MoS_2 and 2H-WS_2 are characterized as structures sorted according to the coordinates of a transition metal.

In general, the results of Raman studies indicate a significant impact of the anisotropy of sizes of graphene-like nanoparticles 2H-MoS_2 and 2H-WS_2, namely in the [110] direction, among nanolayers of S–Mo (W)–S. This blocks the formation of structure-sensitive optical properties and accordingly, affects the characteristics of the semiconductor as a whole.

4. Conclusions

It is established that the Raman spectra of graphene-like 2H-MoS_2 and 2H-WS_2 nanoparticles and their micron particles are closely related. Similarities of the Raman spectra show the homogeneity of graphene-like 2H-MoS_2 and 2H-WS_2 nanoparticles. Small shifts and the Raman spectrum line widening have been observed for graphene-like 2H-MoS_2 and 2H-WS_2 nanoparticles, which are caused by the influence of nanoparticles' sizes. The shifts of Raman bands as functions of the nanoparticle size in the [100] crystallographic direction at equal dimensions in the [013] direction for the 2H-MoS_2 graphene-like nanoparticles, i.e. with the same number of layers of S–Mo—S, have been investigated for the first time. The results of Raman spectroscopy are used for the additional structural certification and the study of vibrational and electronic properties of graphene-like 2H-MoS_2 and 2H-WS_2 nanoparticles.

We thank L.G. Akselrud from Ivan Franko National University of Lviv for X-ray studies of the samples.

1. Z.Y. Zeng, Z.Y. Yin, X. Huang,H. Li, Q. He, G. Lu, F. Boey, and H. Zhang, Angew. Chem. Int. Ed. **50**, 1109 (2011).
2. H. Li, G. Lu, Z. Yin, Q. He, H. Li, Q. Zhang, and H. Zhang, Small **8**, 682 (2012).
3. H. Li,Z. Yin, Q. He, H. Li, X. Huang, G. Lu, D. Fam, A. Tok, Q. Zhang, and H. Zhang, Small ,**8**, 63 (2012).
4. K.S. Novoselov, A.K. Geim, S.V. Morozov, D. Jiang, Y. Zhang, S.V. Dubonos, I.V. Grigorieva, and A.A. Firsov, Science **306**, 666 (2004).
5. K.S. Novoselov, D. Jiang, F. Schedin, T.J. Booth, V.V. Khotkevich, S.V. Morozov,and A.K. Geim, Proc. Natl. Acad. Sci. U.S.A. **102**, 10451 (2005).
6. J.N. Coleman, M. Lotya, A. O'Neill, S.D. Bergin, P.J. King, U. Khan, K. Young, A. Gaucher, S. De *et al.*, Science **331**, 568 (2011).
7. X. Huang,Z. Yin, S.X. Wu, X.Y. Qi, Q.Y. He, Q.C. Zhang, Q.Y. Yan, F. Boey, and H.Zhang, Small **7**, 1876 (2011).
8. B. Radisavljevic, A. Radenovic, J. Brivio, V. Giacometti, and A. Kis, Nat. Nanotechnol. **6**, 147 (2011).
9. X. Huang, X. Qi, F. Boey, and H. Zhang, Chem. Soc. Rev. **41**, 666 (2012).
10. X. Huang, Z. Zeng, Z. Fan, J. Liu, and H. Zhang, Adv. Mater. **24**, 5979 (2012).
11. Q. He, S.X. Wu, Z.Y. Yin, and H. Zhang, Chem. Sci. **3**, 1764 (2012).
12. H. Li, G. Lu, Y. Wang, Z. Yin, C. Cong, Q. He, L. Wang, F. Ding, T. Yu, and H. Zhang, Small **9**, 1974 (2013), doi: 10.1002/smll.201202919.

13. A.C. Ferrari, J.C. Meyer, V. Scardaci, C. Casiraghi, M. Lazzeri, F. Mauri, S. Piscanec, D. Jiang, K.S. Novoselov, S. Roth, and A.K. Geim, Phys. Rev. Lett. **3**, 187401 (2006).
14. R. Saito, M. Hofmann, G. Dresselhaus, A. Jorio, M.S. Dresselhaus, Adv. Phys., **60**, 413 (2011).
15. P.H. Tan, W.P. Han, W.J. Zhao, Z.H. Wu, K. Chang, H. Wang, Y.F. Wang, N. Bonini, N. Marzari, N. Pugno, G. Savini, A. Lombardo, and A.C. Ferrari, Nature Mater. **11**, 294 (2012).
16. S. Najmaei, Z. Liu, P.M. Ajayan, and J. Lou, Appl. Phys. Lett. **100**, 013106 (2012).
17. J.H. Fan, P. Gao, A.M. Zhang, B.R. Zhu, H.L. Zeng, X.D. Cui, R. He, and Q.M. Zhang, J. of Appl. Phys. **115**, 053527 (2014).
18. J.L. Verble, and T.J. Wieting, Phys. Rev. Lett. **25**, 362 (1970).
19. T.J. Wieting, and J.L. Verble, Phys. Rev. B **3**, 4286 (1971).
20. T. Sekine, M. Izumi, T. Nakashizu, K. Uchinokura, and E. Matsuura, J. Phys. Soc. Jpn. **49**, 1069 (1980).
21. T. Sekine, T. Nakashizu, K. Toyoda, K. Uchinokura, and E. Matsuura, Solid State Comm. **35**, 371 (1980).
22. C. Sourisseau, F. Cruege, M. Fouassier, M. Alba, Chem. Phys. **150**, 281 (1991).
23. G. Plechinger, S. Heydrich, J. Eroms, D. Weiss, C. Schuller, and T. Korn, Appl. Phys. Lett. **101**, 101906 (2012).
24. X. Zhang, W.P. Han, J.B. Wu, S. Milana,Y. Lu, Q.Q. Li, A.C. Ferrari, and P.H. Tan, ArXiv 2012, arXiv:1212.6796.
25. A. Molina-Sanchez and L. Wirtz, Phys. Rev. B **84**, 155413 (2011).
26. J.L. Veblde and T.J. Wieting, Phys. Rev. Lett. **25**, 362 (1970).
27. C. Ataca, M. Topsakal, E. Akturk, and S. Ciraci, J. Phys. Chem. C **115**, 16354 (2011).
28. J. Ribeiro-Soares *et al.*, Phys. Rev. B **90**, 115438 (2014).
29. J.L. Veblde and T.J. Wieting, Solid State Comm. **11**, 11941 (1972).
30. C. Lee, H. Yan, L. E. Brus, T. F. Heinz, J. Hone, and S. Ryu, ACS Nano **4**(5), 2695 (2010).
31. J. Verble and T. Wieting, Phys. Rev. Lett. **25**, 362 (1970).
32. G. Frey, R. Tenne, M. Matthews, M. Dresselhaus, and G. Dresselhaus, Phys. Rev. B **60**, 2883 (1999).
33. T. Wieting and J. Verble, Phys. Rev. B, **3**, 4286 (1971).
34. H. Li, Q. Zhang, C.C.R. Yap, B.K Tay, T.H.T. Edwin, A. Olivier, and D. Baillargeat, Adv. Funct. Mater. **22**, 1385 (2012).

Received 23.09.15

А.П. Науменко, Л.М. Куликов, Н.Б. Кьоніг

РАМАНІВСЬКА СПЕКТРОСКОПІЯ
ГРАФЕНО-ПОДІБНИХ НАНОЧАСТИНОК
ДИСУЛЬФІДІВ МОЛІБДЕНА І ВОЛЬФРАМА

Р е з ю м е

Представлено результати дослідження раманівських спектрів графено-подібних наночастинок 2H-MoS_2 та 2H-WS_2, що різняться розмірами в кристалографічних напрямках [013] і [110]. Показано, що раманівські спектри графено-подібних наночастинок та мікронних частинок дисульфіду молібдену якісно подібні. Характерні особливості цих спектрів вказують на гомогенність графено-подібних наночастинок 2H-MoS_2. Вперше показана залежність раманівських спектрів графено-подібних частинок 2H-MoS_2 від їхнього розміру в кристалографічному напрямку [110], тобто положення смуг у спектрі залежить не тільки від кількості шарів S-Mo-S, а й лінійних розмірів базальної площини.